ATLAS NOTE

ATL-COM-PHYS-2011-081

March 15, 2011

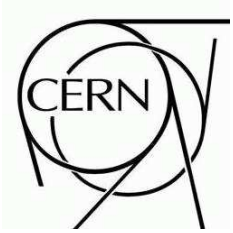

Search for Contact Interactions in Dimuon Events from proton-proton Collisions at $\sqrt{s} = 7$ TeV with the ATLAS detector

The ATLAS Collaboration

Abstract

We discuss the possibility to discover new physics in the ATLAS Detector via a four-fermion contact interaction between two initial-state quarks and two final-state muons. In the absence of new physics signal, we set a 95% C.L. lower limit on the effective scale $\Lambda > 4.9$ TeV (4.5 TeV) for the constructive (destructive) Left-left Isoscalar Model of quark compositeness with integrated luminosity of 42 pb^{-1} at $\sqrt{s} = 7$ TeV.

1 Theoretical Background

Beyond the Standard Model phenomena such as quark/lepton compositeness [1] may be described as a 4-fermion contact interaction (CI) between two incoming quarks and two final state leptons. In the same spirit as the Fermi Interaction described β-decay long before the discovery of the W boson, one can write an effective Lagrangian describing a new interaction without directly knowing the intermediate process [2]:

$$\mathscr{L} = \frac{g^2}{2\Lambda^2}\left[\,\eta_{LL}\left(\bar{\psi}_L\gamma_\mu\psi_L\right)\left(\bar{\psi}_L\gamma^\mu\psi_L\right)\right] + \eta_{RR}\left(\bar{\psi}_R\gamma_\mu\psi_R\right)\left(\bar{\psi}_R\gamma^\mu\psi_R\right) + 2\eta_{LR}\left(\bar{\psi}_L\gamma_\mu\psi_L\right)\left(\bar{\psi}_R\gamma^\mu\psi_R\right)\,\right] \ , \quad (1)$$

where g is a coupling constant and ψ_L (ψ_R) is the left (right) fermionic field. The interaction appears experimentally as a deviation from the Standard Model (SM) dilepton mass spectrum originating from Drell-Yan (DY) production ($q\bar{q} \to \gamma, Z \to l^+l^-$). The value of η (± 1) determines the whether or not the new physics interference is constructive (η =-1) or destructive (η =+1) with the DY in the observable regime. Often for search purposes, the terms in this Lagrangian are treated as different models. For example, the Left-Left Isoscalar Model (LLIM) used in this study is defined by $\eta_{LL} = \pm 1$ and $\eta_{RR} = \eta_{LR} = 0$.

With the introduction of this new interaction (Fig. 1), the differential cross section for the process $q\bar{q} \to \mu^+\mu^-$ is given in terms of the dimuon mass $m_{\mu\mu}$ by

$$\frac{d\sigma}{dm_{\mu\mu}} = \frac{d\sigma_{DY}}{dm_{\mu\mu}} - \eta\frac{F_I}{\Lambda^2} + \frac{F_C}{\Lambda^4} \ , \quad (2)$$

which includes a SM Drell-Yan (DY) term, as well as DY-CI interference (F_I) and pure contact interaction (F_C) terms. Fig. 2 shows the cross section as a function of Λ (note that as $\Lambda \to \infty$ the cross section approaches the DY value). Depending on the model of new physics, there may be different interpretations of the scale Λ. In quark compositeness models, for example, Λ is the scale beneath which fermion constituents are bound to form the SM quarks and leptons.

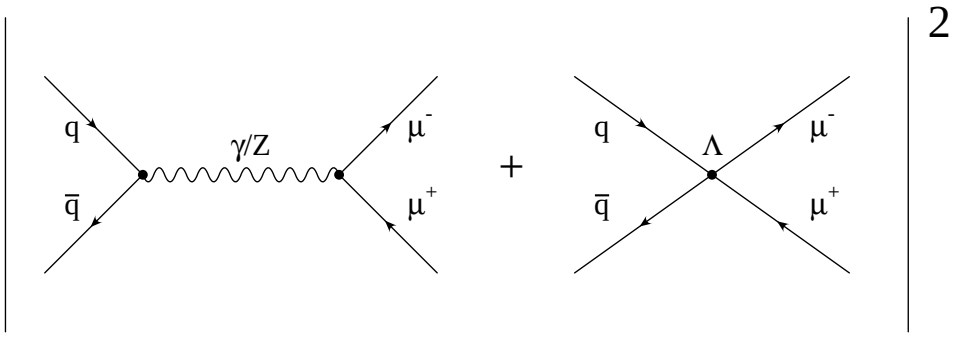

Figure 1: LO production mechanism of Drell-Yan with additional contact term with scale Λ in the dimuon final state.

Previous searches for contact interactions have been carried out in neutrino scattering, as well as at electron-positron, electron-proton and hadron colliders [1]. For the quark-quark-dimuon channel presented here, the best limit in the LLIM is $\Lambda^- > 4.2$ TeV (95% C.L.) for constructive interference and $\Lambda^+ > 2.9$ TeV (95% C.L.) for destructive interference [3].

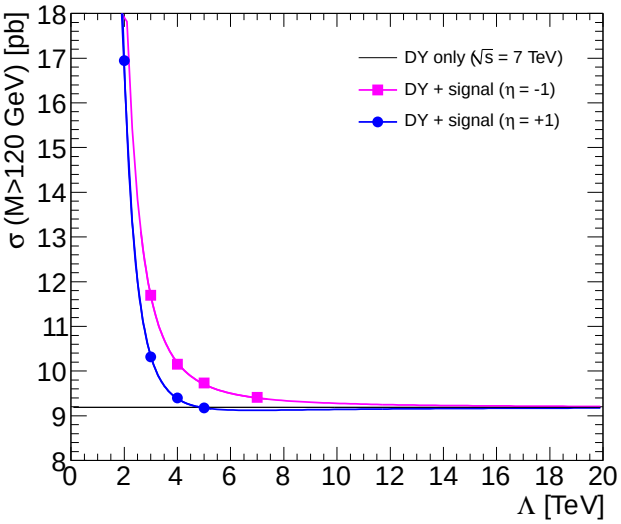

Figure 2: PYTHIA LO cross section ($m_{\mu\mu} > 120$ GeV) as a function of the contact interaction scale Λ.

2 Datasets and Monte Carlo Production

Our dataset consists of the full 2010 run. This corresponds to $\sim$42 pb^{-1} of muon-triggered data, collected with stable beam conditions and fully operational inner detector and muon spectrometer systems.

To model the expected contributions from SM processes, we use leading-order (LO) PYTHIA [4] Monte Carlo event generation and Geant simulation in the ATHENA MC10 framework. We apply data-driven momentum corrections to each individual muon and event-level weighting for multiple vertices according to the same prescription as the Z' analysis, extensively described in [5]. For the main irreducible background, $Z^0/\gamma \to \mu\mu$ (DY), we also account for higher order processes by applying QCD and EW corrections as a function of the true invariant mass. Since the Z^0 peak dominates our statistics, we produce the DY samples in invariant mass bins in order to increase the number of events in the high-mass region. Also included are $Z \to \tau\tau$ and the most dominant non-DY background processes ($t\bar{t}, WW, WZ$ and ZZ) as described in [5], which include muon momentum corrections and vertex pileup event weights applied. Together, these samples as well as the DY make the total background (b).

For our signal (s) samples, four benchmark values for Λ in both the constructive and destructive LLIM have been chosen (Table 1). Like the DY samples, these are also produced in PYTHIA (LO), and contain the DY component as well as the interference and pure CI terms. We require the dimuon invariant mass $m_{\mu\mu} \geq 120$ GeV in the event generation stage to increase statistics above the Z^0 peak where the new physics would appear. In Table 2, we show the production cross section times the branching fraction $BF(X \to \mu\mu)$ for each of the benchmark samples. We also apply all MC corrections to these samples in the same way as they have been applied to the DY MC, with the exception of EW corrections. In this case, since the internal process of the contact term is unknown but the signal sample includes DY as well, an overall shift in the number of expected events is applied corresponding to the difference in DY expected events with and without EW corrections. This is important because we extrapolate the expected number of events as $\Lambda \to \infty$, as we will show later in section 4.1.2. Fig. 3 shows the resulting dimuon invariant mass distribution after event generation, simulation, reconstruction and MC corrections in the two interference models.

All event-level and muon selection criteria are identical to that described in [5]. This includes the following:

- Event-level:

- Event within list of good runs as defined by data quality flags listed in Table 4 of [5]
- Muon-triggered event with trigger listed in Table 5 of [5]
- At least one good primary vertex with $|z(PV)| < 200$mm and three tracks

- Requirements on two muons in the event:
  - Muid combined (author = 12)
  - $pT > 25$ GeV
  - $|\eta| < 2.4$
  - $|z_0| < 1$ mm, $|d_0| < 0.2$ mm with respect to the primary vertex
  - expectBLayerHit=false or numberOfBLayerHits ≥ 1
  - number of pixel hits + number of crossed dead pixel sensors ≥ 2
  - number of SCT hits + number of crossed dead SCT sensors ≥ 6
  - number of pixel holes + number of SCT holes ≤ 1
  - for $|\eta| < 1.9$, require $n_{TRT} > 5$ and $n_{TRT}^{outliers} < 0.9 n_{TRT}$. For $|\eta| \geq 1.9$, accept if $n_{TRT} \leq 5$, and if $n_{TRT} > 5$, then require $n_{TRT}^{outliers} < 0.9 n_{TRT}$. For these cuts, $n_{TRT} = n_{TRT}^{hits} + n_{TRT}^{outliers}$ where the counts on the r.h.s. are mutually exclusive.
  - MS ϕ hits > 0
  - Inner, middle and outer MDT/CSC precision layers with at least 3 hits in each. The MS precision 3-layer requirement should be fulfilled completely in the barrel or in the endcap.
  - Tracks with hits in BEE, EE and BIS78 MS chambers are vetoed
  - Isolated muons in the ID: $\Sigma p_T(\text{cone } 0.3)/p_T < 0.05$

- Finally, the dimuon pair must have:
  - Both muons opposite charge
  - $m_{\mu\mu} \geq 70$ GeV

Table 1: PYTHIA LO Monte Carlo samples for benchmark signals and DY background.

Model	Sample
Constructive interference	
Λ^- = 3 TeV	mc10_7TeV.105863.pythiaContactInt_Lambda3_minus.merge.AOD.e574_s933_s946_r1831_r1700
Λ^- = 4 TeV	mc10_7TeV.105864.pythiaContactInt_Lambda4_minus.merge.AOD.e574_s933_s946_r1831_r1700
Λ^- = 5 TeV	mc10_7TeV.105865.pythiaContactInt_Lambda5_minus.merge.AOD.e574_s933_s946_r1831_r1700
Λ^- = 7 TeV	mc10_7TeV.105608.pythiaContactInt_Lambda7_minus.merge.AOD.e574_s933_s946_r1831_r1700
Destructive interference	
Λ^+ = 2 TeV	mc10_7TeV.105866.pythiaContactInt_Lambda2_plus.merge.AOD.e574_s933_s946_r1831_r1700
Λ^+ = 3 TeV	mc10_7TeV.105867.pythiaContactInt_Lambda3_plus.merge.AOD.e574_s933_s946_r1831_r1700
Λ^+ = 4 TeV	mc10_7TeV.105868.pythiaContactInt_Lambda4_plus.merge.AOD.e574_s933_s946_r1831_r1700
Λ^+ = 5 TeV	mc10_7TeV.105869.pythiaContactInt_Lambda5_plus.merge.AOD.e574_s933_s946_r1831_r1700

For search and limit setting purposes, we define our signal region to be above a reconstructed mass of $m_{\mu\mu} \geq 150$ GeV, and our control region $70 \leq m_{\mu\mu} < 110$ GeV. The acceptance times efficiency of this selection ranges from 35-40% for our contact interaction samples in the signal region, growing inversely

Table 2: Benchmark Λ values with PYTHIA LO cross sections ($\sigma \times BF(X \to \mu\mu)$) for $m_{\mu\mu} \geq$120 GeV with constructive ($\eta = -1$) and destructive ($\eta = +1$) interference.

Λ [TeV]	$\sigma \times BF$ for $\eta = -1$ [pb]	$\sigma \times BF$ for $\eta = +1$ [pb]
2	-	16.94
3	11.69	10.32
4	10.15	9.40
5	9.73	9.18
7	9.41	-
∞ (DY-only)	9.19	

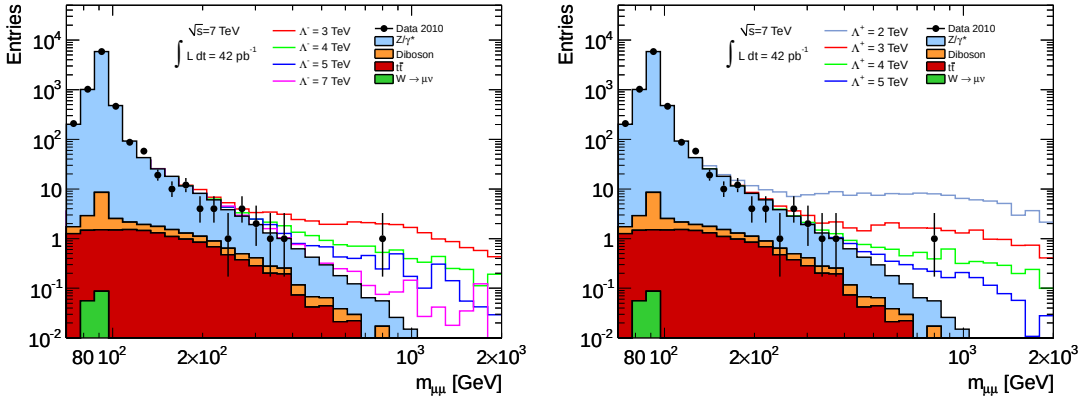

Figure 3: Dimuon mass spectra after reconstruction and event selection for different benchmark Λ values and either constructive interference (left) or destructive interference (right), along with data and dominant SM backgrounds.

to Λ. This is because lower Λ values have increasingly larger production in the high-mass tail of the dimuon spectrum, and these events are produced more centrally within the acceptance of the detector. We use this tight event selection to minimize poorly-reconstructed DY muons, which if mis-measured, could appear as an excess in the tail of the mass spectrum and mimic a signal.

Table 3 shows the number of data events in various mass bins after all selection as well as the expected SM-only events after normalizing to the Z^0 peak in the control region. Table 4 shows the expected number of events after all selection for each signal process (with non-DY backgrounds added) using the same normalization scale.

Table 3: Expected and observed number of events in the dimuon channel. The errors quoted are statistical only.

Mass (GeV)	70-110	150-170	170-200	200-240	240-300	300-400	400-550	550-800	800-1200	1200-2000
DY	7547 ± 7	17.19 ± 0.33	12.77 ± 0.29	7.81 ± 0.22	5.05 ± 0.11	2.49 ± 0.04	0.99 ± 0.01	0.29 ± 0.00	0.06 ± 0.00	0.01 ± 0.00
$t\bar{t}$	5.96 ± 0.22	1.24 ± 0.04	1.22 ± 0.03	1.03 ± 0.03	0.73 ± 0.02	0.37 ± 0.01	0.11 ± 0.00	0.02 ± 0.00	0.00 ± 0.00	0.00 ± 0.00
Diboson	10.06 ± 0.14	0.48 ± 0.04	0.41 ± 0.03	0.28 ± 0.03	0.24 ± 0.02	0.16 ± 0.02	0.06 ± 0.01	0.02 ± 0.01	0.01 ± 0.00	0.00 ± 0.00
W+jets	0.25 ± 0.17	0.00 ± 0.00	0.00 ± 0.00	0.00 ± 0.00	0.00 ± 0.00	0.00 ± 0.00	0.00 ± 0.00	0.00 ± 0.00	0.00 ± 0.00	0.00 ± 0.00
Total	7563 ± 7	18.92 ± 0.34	14.40 ± 0.29	9.12 ± 0.23	6.02 ± 0.11	3.03 ± 0.05	1.16 ± 0.02	0.33 ± 0.01	0.07 ± 0.00	0.01 ± 0.00
Data	7563	11	11	7	6	2	0	1	0	0

Table 4: Expected number of events in the presence of new physics for various contact interaction scales with constructive (Λ^-) and destructive (Λ^+) interference. The errors quoted are statistical only.

Mass (GeV)	150-170	170-200	200-240	240-300	300-400	400-550	550-800	800-1200	1200-2000
Λ^- = 3 TeV	19.14 ± 0.46	15.73 ± 0.41	11.22 ± 0.35	8.47 ± 0.30	7.89 ± 0.30	6.01 ± 0.26	6.50 ± 0.27	5.11 ± 0.24	2.97 ± 0.17
Λ^- = 4 TeV	18.79 ± 0.43	14.27 ± 0.37	10.01 ± 0.31	6.54 ± 0.24	5.04 ± 0.22	3.03 ± 0.17	2.27 ± 0.15	1.45 ± 0.12	1.08 ± 0.09
Λ^- = 5 TeV	17.44 ± 0.39	14.25 ± 0.36	9.40 ± 0.29	6.17 ± 0.24	4.33 ± 0.20	1.95 ± 0.13	1.29 ± 0.11	0.72 ± 0.08	0.36 ± 0.055
Λ^- = 7 TeV	17.32 ± 0.39	13.84 ± 0.35	9.26 ± 0.28	6.30 ± 0.23	3.26 ± 0.17	1.26 ± 0.10	0.58 ± 0.07	0.21 ± 0.04	0.11 ± 0.031
Λ^+ = 2 TeV	21.64 ± 0.59	19.31 ± 0.55	15.80 ± 0.50	15.22 ± 0.50	21.23 ± 0.60	21.60 ± 0.60	25.46 ± 0.64	21.41 ± 0.58	15.05 ± 0.46
Λ^+ = 3 TeV	18.59 ± 0.43	15.18 ± 0.39	10.05 ± 0.31	7.19 ± 0.26	5.45 ± 0.23	4.59 ± 0.21	5.27 ± 0.23	4.29 ± 0.20	3.07 ± 0.17
Λ^+ = 4 TeV	18.16 ± 0.40	14.29 ± 0.35	8.81 ± 0.27	6.05 ± 0.23	3.62 ± 0.18	2.10 ± 0.14	1.59 ± 0.12	1.52 ± 0.12	0.84 ± 0.08
Λ^+ = 5 TeV	18.48 ± 0.40	13.62 ± 0.34	8.84 ± 0.27	5.44 ± 0.21	2.91 ± 0.15	1.61 ± 0.12	0.88 ± 0.09	0.53 ± 0.07	0.28 ± 0.05

3 Consistency of Data with Standard Model Simulation

One way to visually check whether or not there is an excess of events present in our data sample is to draw the integral from $m_{\mu\mu} \to \infty$ as a function of $m_{\mu\mu}$. Fig. 4 shows no indication of an excess.

In order to quantify this agreement, we construct a binned log-likelihood ($-ln(L)$) test between our dataset and the expected number of events from SM-only processes. Calculating the Poisson probability between the total number of events observed in data and SM-expected events in each mass bin, we find $-ln(L)$ =10.7. 100k pseudo-experiments were performed to determine the negative log-likelihood between the nominal SM and a random Poisson fluctuations independently each mass bin. Fig. 5 shows the resulting distribution, with an arrow indicating the $-ln(L)$ value found in data. By integrating this pseudo-experiment distribution from the observed value to infinity, we find a p-value of 56%, thus showing consistency with the SM.

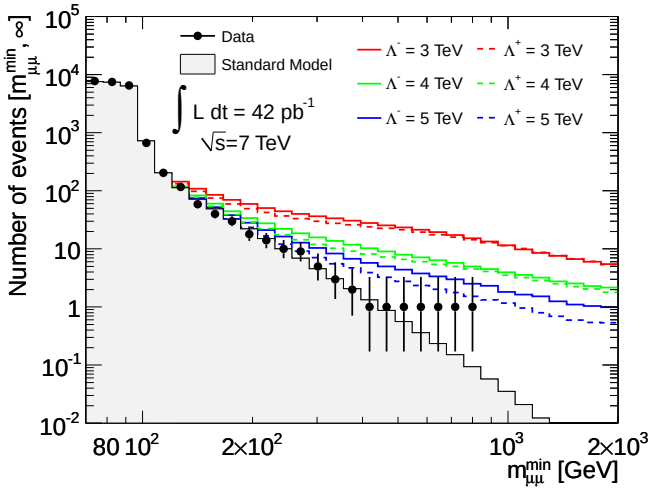

Figure 4: Integral of $m_{\mu\mu} \to \infty$ as a function of $m_{\mu\mu}$ for data, SM-only, and various contact interaction samples.

4 Bayesian Limit-setting

As we have ruled out the presence of new physics in our data set, we use a Bayesian counting method in order to set a limit on Λ in the absence of observed signal. In general, one can construct the likelihood in N_k invariant mass bins for $\bar{n}$ observed events given expected signal and background events (s and b, respectively) as:

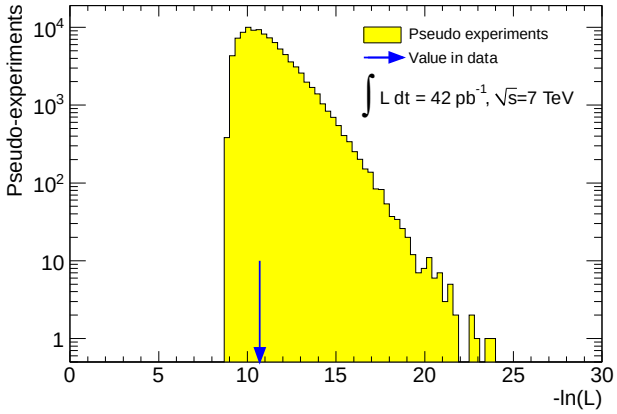

Figure 5: Negative log-likelihood distribution resulting from pseudo-experiments with fluctuations on the number of expected SM-only events. The value in data was found to be 10.7, with p-value = 56%.

$$\mathscr{L}(\bar{n} \mid \theta, \bar{\nu}) = \prod_{k=1}^{N_k} \frac{\mu_k^{n_k} e^{-\mu_k}}{n_k!}, \quad \text{where} \quad \mu_k = s(\theta, \nu_k) + b(\nu_k). \tag{3}$$

Here, θ is a parameter characterizing the new physics on which we would like to set the limit, and $\bar{\nu}$ encompasses the "nuisance" parameters (for example resolution, efficiency, etc) which are not directly measured. The Poisson distribution in the product can be approximated with a Gaussian function for sufficiently large number of observed events in mass bin k ($n_k \geq 40$).

According to Bayes' Theorem, the posterior probability density function (PDF) of the parameter θ given $\bar{n}$ and $\bar{\nu}$ can be written as:

$$\mathscr{P}(\theta \mid \bar{n}, \bar{\nu}) = \frac{1}{Z} \mathscr{L}(\bar{n} \mid \bar{\theta}, \bar{\nu}) P(\theta, \nu), \tag{4}$$

where Z normalizes the posterior PDF as a function of θ. $P(\theta, \nu)$ is the prior probability function depending on θ, which should be a function of our new contact interaction scale Λ and the nuisance parameters ν. The latter may be marginalized by convolving each Poisson probability with a prior probability function (typically chosen as Gaussian). For one particular mass bin, the likelihood would then look like:

$$\mathscr{L}(\bar{n} \mid \theta, \nu) = \frac{1}{C} \int_0^\infty \frac{\mu'^n e^{-\mu'}}{n!} e^{-\frac{(\nu-\nu')^2}{2\sigma_\nu^2}} d\nu' \ . \tag{5}$$

Note that the parameter μ' can depend on ν.

The 95% C.L limit is then found by integrating over the posterior PDF and solving for θ_{lim}:

$$\int_0^{\theta_{lim}} \mathscr{P}(\theta' \mid \bar{n}, \bar{\nu}) d\theta' = 0.95. \tag{6}$$

4.1 Contact Interaction Limit Setting

Often when setting a limit one can treat the signal and background contributions separately, such as in the case of a resonance search [6]. However, because new physics via the contact interaction would have appeared as a continuous excess of events above the expected DY invariant mass distribution, and the signal interference with DY component of the background contributes a non-negligible amount to this excess, we choose to employ a slightly different method than that of the $Z' \to \mu\mu$ search.

4.1.1 Choice of Prior

The prior in Eq. 4 can be factored as $P(\theta,\nu) = P(\theta)P(\nu)$. Ideally we would like to choose $P(\theta)$ to be flat in the observable parameter θ. Since the interference term in Eq. (2) dominates as $\Lambda \to \infty$, we choose a prior of the form

$$\theta = \frac{1}{\Lambda^2}. \tag{7}$$

Typically, this is the prior chosen for contact interaction searches.

$P(\nu)$ is taken as a Gaussian with width dN_{exp}, representing the effect of systematic uncertainties to be discussed later in the text. The posterior dependence on ν is integrated out by sampling from $P(\nu)$ in each mass bin 50,000 times (enough to cover the Gaussian-distributed systematics' phase space).

4.1.2 Limit Setting Method and Results

We can write Eq. (3) using n_k = number of events observed in data in a given invariant mass bin k and $\mu_k = N_k^{\exp}(\theta,\nu_k)$, the number of expected events in each mass bin in the presence of new physics. We have chosen 9 mass bins with limits of $M_{\mu\mu}$ = 150, 170, 200, 240, 300, 400, 550, 800, 1200 and 2000 GeV (Fig. 6) and calculated the expected number of events after normalizing the distribution in the control region. To provide more values of N^{exp} to be used in the construction of the posterior PDF, we fit the number of expected events in each bin according to

$$N^{exp}(\Lambda) = c_0 + \frac{c_1}{\Lambda^2} + \frac{c_2}{\Lambda^4} \quad . \tag{8}$$

The fits for both constructive and destructive interference are shown in Fig. 7.

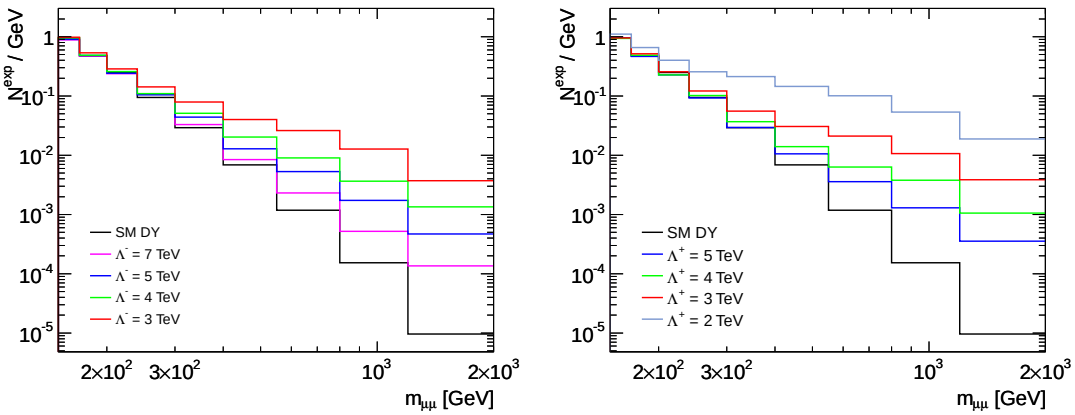

Figure 6: Number of expected events as a function of invariant mass for constructive (left) and destructive (right) interference models, normalized to the bin width.

For for the expected limit, we take the number of SM-only background events b_k as the number of observed events from MC in each mass bin. The posterior PDF with marginalized systematics is drawn as a function of θ which takes the prior discussed in section 4.1.1 into account. Without systematics, the integral of the normalized posterior PDF in Eq. (6) with $\theta = \frac{1}{\Lambda^2}$ yields an expected limit of Λ^-_{lim} = 5.2 TeV for constructive interference and Λ^+_{lim} = 4.9 TeV for destructive interference (both at 95% C.L.). Fig 8 shows the expected posterior PDF distributions from MC for SM-only and in the presence of a Λ^- = 5 TeV constructive interference signal. In the latter case, there would be a clear preference at $\frac{1}{\Lambda^2}$ = 0.04 [TeV^{-2}].

In order to determine the range of the expected limit within statistical fluctuations, 5000 pseudo-experiments were performed, varying N_i events in each bin by a random Poisson amount. The resulting

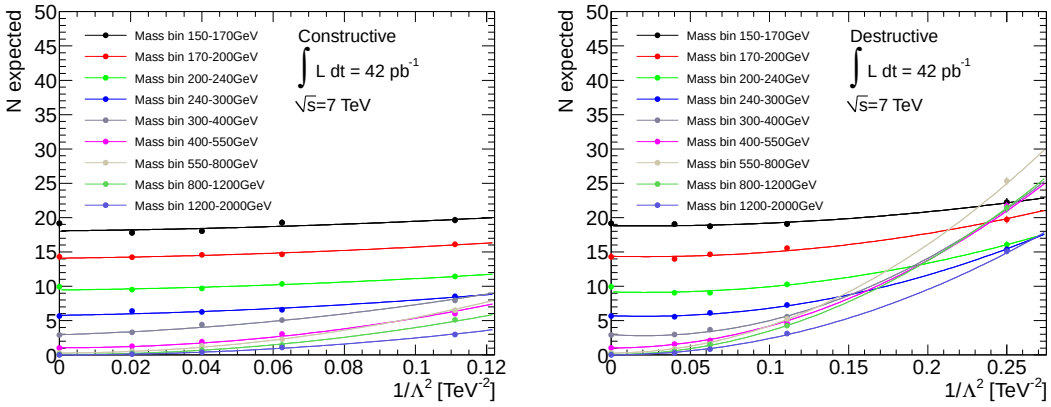

Figure 7: Quadratic fits in each mass bin for the constructive (left) and destructive (right) interference models as a function of $\frac{1}{\Lambda^2}$, with benchmark Λ values shown as points.

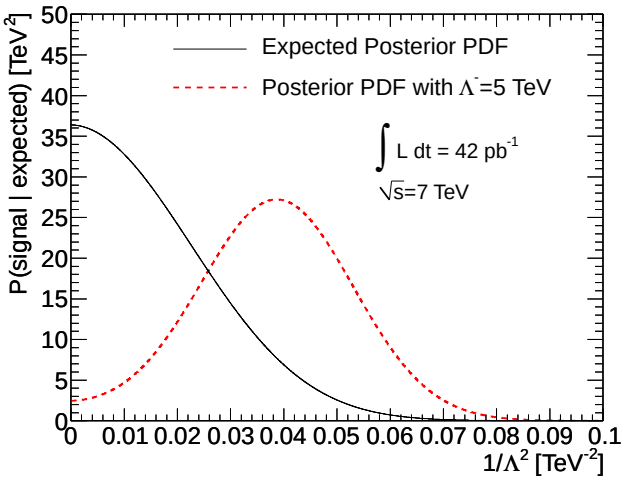

Figure 8: Showing the expected posterior PDF from MC for SM-only and in the presence of new physics at $\Lambda^- = 5$ TeV.

width of the Gaussian fit to this distribution yields a 0.3 TeV width on the expected limit for both constructive and destructive interference (Fig. 9).

From data, we extract an observed limit of $\Lambda^-_{lim} = 5.1$ TeV for constructive interference and $\Lambda^+_{lim} = 4.6$ TeV for destructive interference (at 95% C.L.) without systematic uncertainties incorporated, well within range of the expected limits.

After including systematics (see section 4.1.3 below), we find an expected limit of $\Lambda_{lim} = 5.1$ TeV (4.8 TeV) and an observed limit in data of $\Lambda_{lim} = 4.9$ TeV (4.5 TeV) for constructive (destructive) interference at 95% C.L. The posterior distributions are shown in Fig. 10 for both the expected and observed limits.

4.1.3 Details of the Treatment of Systematic Uncertainties

Because we normalize to the Z^0 peak, only mass-dependent systematic uncertainties affect our limit calculation, and any overall constant scale to each uncertainty factors out. Statistical uncertainty dominates with low luminosity, so we have chosen to take the conservative estimates of theoretical and detector systematics described in [5]. The systematics are summarized in Table 5, and with the exception of the

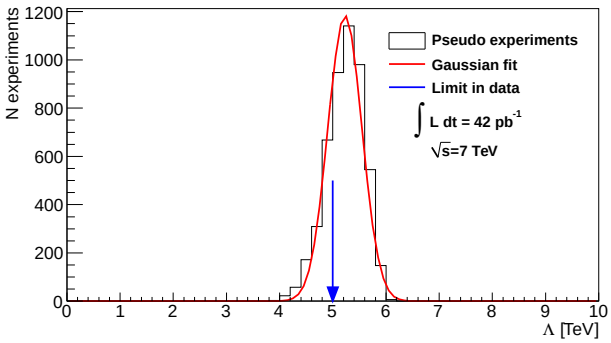

Figure 9: Result of pseudo-experiments on the expected limit. The mean of the fitted Gaussian is (5.23±0.01) TeV and the width is (0.321±0.003) TeV.

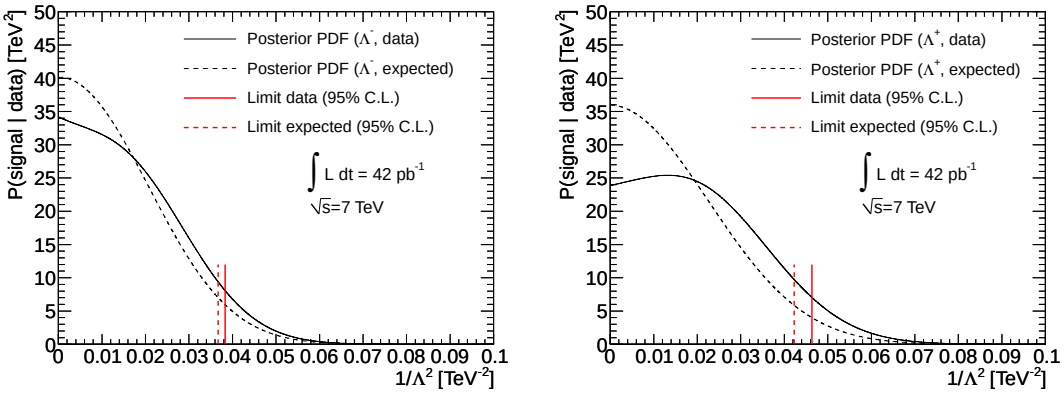

Figure 10: Expected and observed posterior PDF distributions for constructive (left) and destructive (right) interference.

muon momentum resolution uncertainty, each of these were taken as linear functions of $m_{\mu\mu}$ starting at the Z^0 peak and rising to $\pm$ the value obtained at $m_{\mu\mu}$ = 1 TeV. The effect of the momentum resolution uncertainty was assessed by taking the full magnitude of the muon momentum correction to the MC mentioned in Section 2 as the systematic uncertainty. This was found by fitting the ratio of invariant mass distributions with and without muon momentum corrections with a second order polynomial (Fig. 11). The values of this function at the Z^0 peak and at $m_{\mu\mu}$ = 1 TeV are also shown in Table 5.

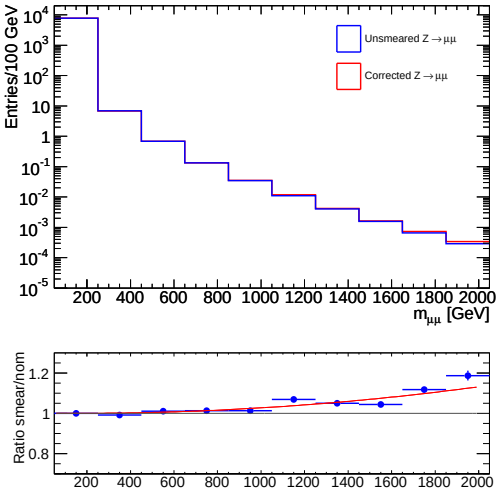

Figure 11: DY distributions before and after muon resolution smearing corrections. Though a small effect, the ratio between smeared/nominal shows a $\sim$ 10% difference at 2 TeV.

During the creation of the invariant mass distributions, each systematic uncertainty was applied individually as an event weight either as a function of true mass (in the case of K-factor and PDF uncertainties) or reconstructed mass (in the case of muon efficiency and momentum resolution uncertainties).

With each systematic individually fluctuated up and down, we create a family of invariant mass distributions for each MC sample. Note that not all systematics are applied to every sample (as listed in Table 5). The difference between the expected number of events for each systematic uncertainty in k mass bins $dN_\Lambda^{i,k} = (N^k_{systematic} - N^k_{nominal})^i_\Lambda$ was calculated on the i^{th} systematic for both the full SM-only background and the benchmark signal samples separately using both upwards and downwards fluctuations. Taking the larger of either the up or down fluctuation for dN_i, the systematics in each mass bin were added in quadrature: $dN^k_\Lambda = (dN_1 \oplus dN_2 \oplus ... \oplus dN_i)^k_\Lambda$. Here, we also consider an additional systematic in the extrapolation fit of N_{exp} by adding the MC statistical uncertainty of signal samples in each mass bin in quadrature to dN^k_Λ (these values are quoted in Table 4). Finally dN^k was fit in each mass bin as a function of $1/\Lambda^2$ to extrapolate between the benchmark signal values (Fig. 12). The value of dN^k at a particular $1/\Lambda^2$ becomes the width of the Gaussian prior in Eq. 5 in each mass bin (and dN^k_b, the value for SM-only, is used for the p-value and expected limit range calculations). Table 6 shows the limit with and without adding systematic uncertainties. The effect is smaller than the statistical range of the limit shown in Fig. 9, with an observed limit difference of 0.17 TeV for constructive interference and 0.14 TeV for destructive interference.

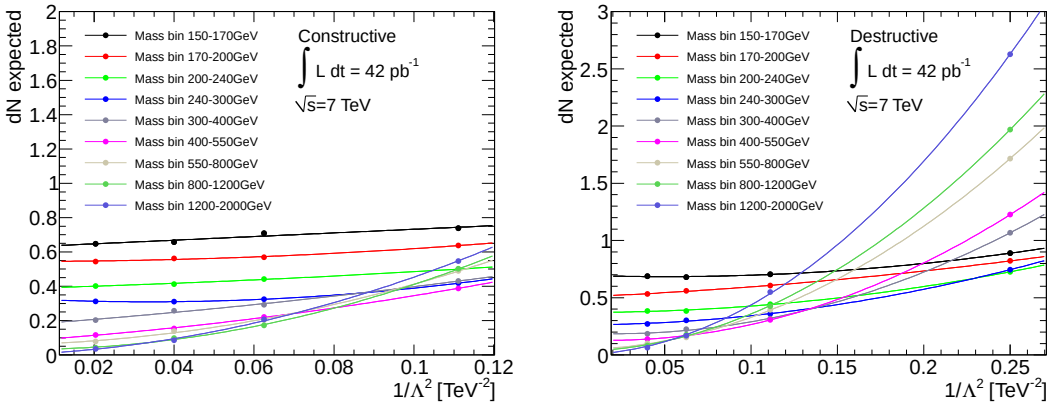

Figure 12: 2^{nd}-order polynomial fits to dN in each mass bin for the constructive (left) and destructive (right) interference models as a function of $\frac{1}{\Lambda^2}$, with benchmark Λ values shown as points. Note that the total systematic uncertainty for background only ($\frac{1}{\Lambda^2} = 0$) was not used in this fit because the DY systematics were treated differently than for the signal samples.

Table 5: Systematic uncertainty on N_{exp} at $M_{\mu\mu} = 1$ TeV. All systematics have a linear dependence on mass, with the exception of muon momentum resolution which has a quadratic dependence. The MC samples on which each of these are applied are shown.

Systematic	value at Z^0	at 1 TeV	Signal	DY-only	Other BGs
Trigger and Reconstruction Efficiency	0.3%	3%	✓	✓	✓
Muon momentum resolution	0.01%	2.7%	✓	✓	✓
PDF Uncertainty	3%	6%	✓	✓	
QCD K-factor	0.3%	3%	✓	✓	
EW K-factor	0.4%	4.5%		✓	

5 Conclusions

With the full 2010 data set, we are able to set limits on the 4-fermion contact interaction $q\bar{q} \to \mu^+\mu^-$ in the LLIM model, for both constructive and destructive interference:

$$\Lambda^- > 4.9 \text{ TeV (95\% C.L.)} \quad (9)$$

$$\Lambda^+ > 4.5 \text{ TeV (95\% C.L.)} \quad (10)$$

These are the best limits to date.

Table 6: Expected and observed lower limits on Λ with and without systematic uncertainties. The 2^{nd} decimal place is shown to illustrate the change with the addition of systematics.

	Expected Limit (TeV)		Observed Limit (TeV)	
	Constructive	Destructive	Constructive	Destructive
Without Systematics	5.22	4.86	5.11	4.64
Including Systematics	5.14	4.82	4.94	4.50

References

[1] K. Nakamura *et al.* (Particle Data Group), J. Phys. G **37**, 075021 (2010).

[2] E. Eichten, K. Lane, and M. Peskin, “New Tests for Quark and Lepton Substructure”, Phys. Rev. Lett. 50 11 811-814, 1983.

[3] K. Abe *et al.* (CDF Collaboration), Phys. Rev. Lett. **79**, 2198 (1997).

[4] T. Sjöstrand, P. Edén, C. Friberg, L. Lönnblad, G. Miu, S. Mrenna and E. Norrbin, Computer Phys. Commun. 125 238 (LU TP 00-30, hep-ph/0010017, 2001.

[5] ATLAS Exotics Dimuon support note, ATL-COM-PHYS-2011-084, 2011.

[6] ATLAS Exotics Dilepton statistics note, ATL-COM-PHYS-2011-085, 2011.

[7] G. Aad *et al.* (ATLAS Collaboration), “Expected Performance of the ATLAS Experiment, Detector, Trigger and Physics”, CERN-OPEN-2008-020, 2008.

[8] G. Aad *et al.* (ATLAS Collaboration), “The ATLAS Experiment at the CERN Large Hadron Collider”, Journal of Instrumentation 3 08 S08003, http://stacks.iop.org/1748-0221/3/S08003, 2008.

[9] Thompson, E N, Willocq, S, Black, K M,“Search for Contact Interactions in the Dimuon Final State at ATLAS”, DPF’09 talk proceedings (http://arxiv.org/abs/0910.3384), October 2009.